CHEMISTRY
A EUROPEAN JOURNAL

DOI: 10.1002/chem.200600369

Electrochromic Hysteresis Performance of a Prussian Blue Film Arising from Electron-Transfer Control by a Tris(2,2′-bipyridine)ruthenium(II)-Doped WO_3 Film as Studied by a Spectrocyclic Voltammetry Technique

Koji Sone, Kanae Konishi, and Masayuki Yagi*[a]

Abstract: A $[Ru(bpy)_3]^{2+}$ (bpy = 2,2′-bipyridine)-doped WO_3 film was prepared as a base layer on a substrate by cathodic electrodeposition from a colloidal triad solution containing peroxotungstic acid (PTA), $[Ru(bpy)_3]^{2+}$, and poly(sodium 4-styrenesulfonate) (PSS). A Prussian blue (PB; Fe^{II}-Fe^{III}) film was cathodically electrodeposited on the $[Ru(bpy)_3]^{2+}$-doped WO_3 film or neat WO_3 film from an aqueous Berlin brown (BB; Fe^{III}-Fe^{III}) colloid solution to yield a $[Ru(bpy)_3]^{2+}$-doped WO_3/PB bilayer film or WO_3/PB bilayer film. For the spectrocyclic voltammogram (SCV) of the WO_3/PB film, a redox response of Prussian white (PW; Fe^{II}-Fe^{II})/PB was observed at 0.11 V, however, further oxidation of PB to BB was not allowed by the interfacial n-type Schottky barrier between the WO_3 and PB layers. For the $[Ru(bpy)_3]^{2+}$-doped WO_3/PB film, any electrochemical response assigned to the redox of PB was not observed in the cyclic voltammogram, however, the in situ absorption spectral change recorded simultaneously showed the significant redox reactions based on PB. The SCV revealed that PW on the $[Ru(bpy)_3]^{2+}$-doped WO_3 film is completely oxidized to PB by a geared reaction of Ru^{II}/Ru^{III} at 1.05 V, and that 32% of PB formed is further oxidized to BB by the same geared reaction in the potential scan to 1.5 V. PB was completely re-reduced to PW by a geared reaction of H_xWO_3/WO_3 at −0.5 V in the reductive potential scan. These geared electrochemical reactions produced an electrochromic hysteresis performance of the PB film layered on the $[Ru(bpy)_3]^{2+}$-doped WO_3 film.

Keywords: electrochemistry · electron transfer · Prussian blue · redox chemistry · ruthenium complexes

Introduction

There is considerable interest in fundamental interfacial chemistry at heterojunctions between semiconductors and electrolyte solutions.[1–4] There have been extensive studies in n-type semiconductors, such as TiO_2, ZnO, WO_3, and CdS, and the formation of space-charge layers in interface heterojunctions (so called Schottky junctions)[1] has been demonstrated. In this type of the heterojunction, the energy barrier (Schottky barrier) of the space-charge layer does not allow redox species in solutions to be oxidized at the interface at potential levels above the flat band (FB) potential of n-type semiconductors. Dye-sensitized solar cells have been studied recently, in which ruthenium or organic dyes are adsorbed on the surface of TiO_2 and an ultrafast electron injection from the excited state of the dyes to the conduction band of TiO_2 occurs at the liquid heterojunction to achieve solar-energy conversion.[5,6] The progress in this research field has developed new fundamentals and unique application of interfacial liquid heterojunctions doped (in a broad meaning) by functional molecules.

WO_3 is an inexpensive n-type semiconductor,[7,8] and owing to its distinct electrochromic property in electrochemical reduction with intercalation of cations (H^+ or Li^+), it is also useful for electrochromic devices and chemical sensors.[9–11] Doping of functional molecules to a bulk or an interface of WO_3 could expand its functions and applications to include a large variety of electronic or photoelectronic devices. $[Ru(bpy)_3]^{2+}$ (bpy = 2,2′-bipyridine) is attracting much attention for its potential ability regarding electro- and photochemical reactions.[12] It is a stable redox molecule with an intense absorption band at 453 nm assigned to metal-to-ligand charge transfer (MLCT)[12] that is reversibly eliminated by oxidation to $[Ru(bpy)_3]^{3+}$. In recent work,

[a] K. Sone, K. Konishi, Prof. Dr. M. Yagi
Faculty of Education and Human Sciences and
Center for Transdisciplinary Research, Niigata University
8050 Ikarashi-2, Niigata 950-2181 (Japan)
Fax: (+81) 25-262-7151
E-mail: yagi@ed.niigata-u.ac.jp

Supporting information for this article is available on the WWW under http://www.chemeurj.org/ or from the author: In situ absorption spectral changes and cyclic voltammetry data.

$[Ru(bpy)_3]^{2+}$ was doped in a WO_3 film by cathodic electrodeposition from an aqueous colloidal triad solution containing peroxotungstic acid (PTA), $[Ru(bpy)_3]^{2+}$, and poly(sodium 4-styrenesulfonate) (PSS).[13,14] In the absence of PSS, precipitation is formed by electrostatic interaction between the cationic $[Ru(bpy)_3]^{2+}$ and anionic PTA. Remarkably, PSS suppresses the precipitation to provide a stable colloidal triad solution that is favorable for electrodeposition. For the $[Ru(bpy)_3]^{2+}$-doped WO_3 film, an ohmic contact is formed at the interface between WO_3 and $[Ru(bpy)_3]^{2+}$, though a Schottky heterojunction remains at the interface between WO_3 and an aqueous solution. This very unusual electrochemical feature cannot be observed in any other films, including a WO_3/$[Ru(bpy)_3]^{2+}$ film prepared by solvent evaporation from WO_3 suspension containing $[Ru(bpy)_3]^{2+}$. It allows the redox of Ru^{II}/Ru^{III} to occur at the potential (1.03 V vs saturated calomel electrode (SCE)) above the FB potential (0.26 V) of WO_3.[13] We are interested in this unusual electrochemical feature because it could function as an electron-transfer channel passing through the Schottky barrier at the WO_3 heterojunction.

Prussian blue (PB) is a stable macromolecule composed of a repeating unit of $Fe_4^{III}[Fe^{II}(CN)_6]_3$ with an intense absorption band at 718 nm assigned to intervalence charge transfer (IVCT) of Fe^{III}-NC-Fe^{II}.[15–17] Because of significant decreases in the absorption band by reduction to Prussian white (PW) or oxidation to Berlin brown (BB), a PB film is a potential electrochromic material.[18,19] Here, we present a new electrochromic $[Ru(bpy)_3]^{2+}$-doped WO_3/PB bilayer film. Electron-transfer reactions on the bilayer film were studied by using a spectrocyclic voltammetry (SCV) technique, illustrating that PW is oxidized to PB by a geared reaction of Ru^{II}/Ru^{III} and PB is re-reduced to PW by a geared reaction of H_xWO_3/WO_3. A unique and first electrochromic hysteresis performance based on PW/PB is produced by the geared cycle redox reactions of the $[Ru(bpy)_3]^{2+}$-doped WO_3/PB film.

Results and Discussion

PB film: Figure 1 shows a cyclic voltammogram (CV) of an aqueous colloid solution of BB measured by using a bare indium tin oxide (ITO) electrode. During a reductive scan from 1.5 V, a cathodic wave was observed at 0.57 V, followed by a relatively large cathodic wave at −0.08 V. The former is assigned as reduction of BB to deposit a PB film onto the ITO electrode, and the latter as the subsequent reduction of the deposited PB film to the PW film. During a reverse oxidative scan, two anodic peaks were observed at 0.35 and 1.10 V, indicating oxidation processes of PW to PB films and PB to BB films, respectively.

CV of the PB film electrodeposited (5 mC cm^{-2}) onto an ITO electrode was measured in a 0.1 M KNO_3 aqueous solution (pH 3.0) and exhibited two well-defined redox responses of PW/PB and PB/BB at 0.14 V and 0.86–1.10 V vs SCE, respectively, in the range of −0.4–1.4 V, as shown by the solid line in Figure 2. The redox reactions of the PB film are summarized in Equation (1):

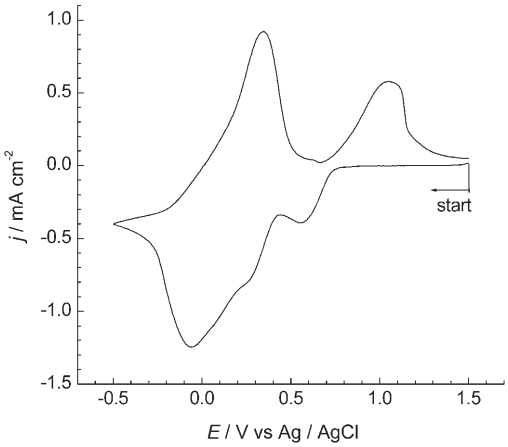

Figure 1. CV of a 10 mM Berlin brown (BB; Fe^{III}-Fe^{III}) aqueous solution measured at 50 mV s^{-1} by using an ITO electrode.

$$Fe^{II}\text{-}Fe^{II}\ (PW) \underset{0.14\ V}{\overset{-e^-}{\rightleftharpoons}} Fe^{II}\text{-}Fe^{III}\ (PB) \underset{0.86-1.10\ V}{\overset{-e^-}{\rightleftharpoons}} Fe^{III}\text{-}Fe^{III}\ (BB) \quad (1)$$

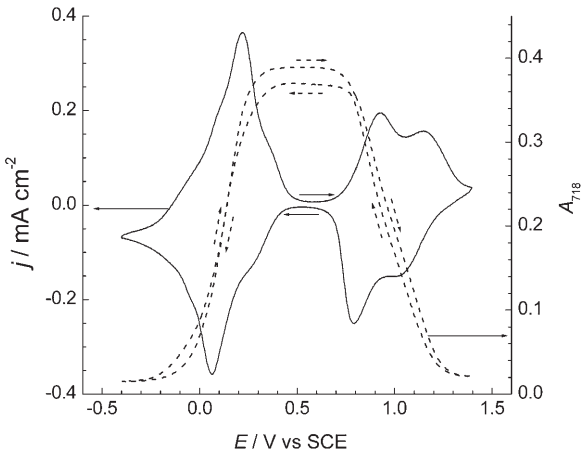

Figure 2. CV (solid line) and absorbance change at 718 nm (A_{718}; dashed line) in a SCV measurement of a PB film in 0.1 M KNO_3 aqueous solution (pH 3.0), measured at 20 mV s^{-1}.

The in situ visible-absorption spectral change recorded simultaneously during CV measurement is shown in Figure 3 (three-dimensional representation) and in Supporting Information Figure S1 (two-dimensional representation, segmented into each reaction stage). At −0.4 V of an applied potential, the film is in a PW state with very weak absorption in the visible region. During an oxidative scan from −0.4 to 0.4 V, an intense absorption band at 718 nm increased due to PB formation by oxidation of PW, and in a successive scan to 1.4 V, it decreased as a second absorption band at 417 nm increased due to oxidation of PB to BB. The spectral

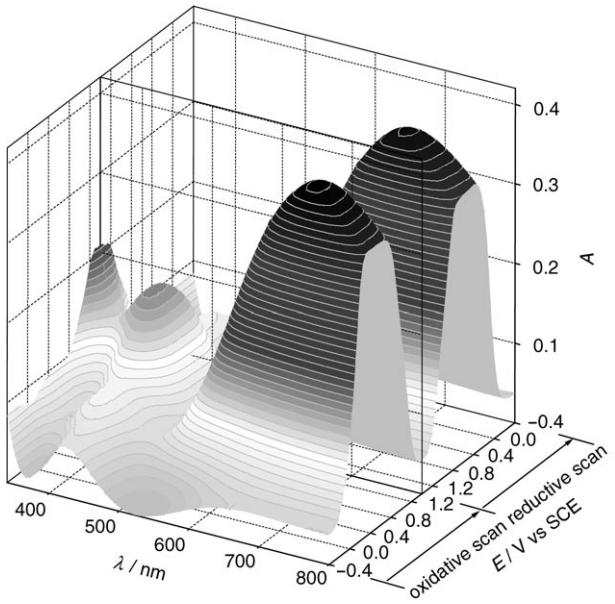

Figure 3. In situ absorption spectral change in a SCV measurement of a PB film in 0.1 M KNO_3 aqueous solution (pH 3.0), measured at 20 mV s^{-1}.

change was shown to be reversible by a reverse reductive scan from 1.4 to −0.4 V. The potential profile of absorbance at 718 nm (A_{718}) is depicted on the CV in Figure 2. Two reversible changes of A_{718} at 0.1 and 1.0 V are synchronized with the electrochemical responses of PW/PB and PB/BB, respectively, indicating that the absorbance change occurs in response to the electrochemical reactions. The amount of electroactive PB (Γ_{PB}) was calculated from the anodic peak area at 0.22 V to be 5.9×10^{-8} mol cm^{-2}. The molar absorption coefficient of the PB film (ε_{PB}) at 718 nm was calculated to be 6600 $M^{-1}cm^{-1}$ by applying Equation (2), based on a Lambert–Beer law, in which $A_{718}=0.39$ and Γ_{PB} is the value quoted above:

$$A_{718} = \varepsilon_{PB}\,\Gamma_{PB} \times 10^3 \qquad (2)$$

The ε_{PB} is consistent with literature values (5800–7900 $M^{-1}cm^{-1}$).[15,18]

WO_3/PB film: A CV of a WO_3 film in a 0.1 M KNO_3 aqueous solution is shown in Figure 4a, in which the redox response of H_xWO_3/WO_3 was observed below the FB potential (0.26 V) of the WO_3 film. The absence of an electrochemical response above the FB potential is a typical rectification property for n-type semiconductors in aqueous solution. Figure 4b shows a CV of the WO_3 film on the electrode in a 10 mM BB aqueous solution. In a reductive scan from 1.5 to 0.26 V, BB colloid was not reduced to PB because of the Schottky barrier at the interface between the WO_3 film and the electrolyte solution. This suggests that BB colloid can not diffuse in the WO_3 film to the ITO surface for the direct electrochemical reaction. The high cathodic current rose at 0.26 V of the FB potential of WO_3. This can be assigned as multiple reduction processes of BB colloid to deposit the

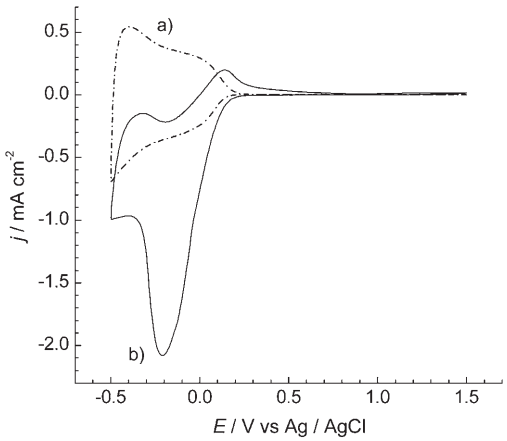

Figure 4. CVs of a WO_3 film in 0.1 M KNO_3 aqueous solution (a) and in 10 mM BB aqueous solution (b), measured at 50 mV s^{-1}.

PB film, and the subsequent reduction of this to the PW film. Both reduction processes occur through H_xWO_3, reduced electrochemically below the FB potential. It is inferred from the results that the PB film must be layered on the basal WO_3 film.

An absorption spectrum of the WO_3/PB film exhibited an absorption maximum at 727 nm due to PB, which is a little different from that prepared on the ITO electrode. The repeating structure of the PB film might be slightly disordered upon deposition on the WO_3 film. The absorbance at 727 nm (A_{727}) was 0.44 for the film prepared by electrodeposition to 10 mC cm^{-2}. The Γ_{PB} for the WO_3/PB film was calculated to be 6.7×10^{-8} mol cm^{-2} according to Equation (2), in which $A_{727}=0.44$ and $\varepsilon_{PB}=6600$ $M^{-1}cm^{-1}$ (at 718 nm) for the PB film, as calculated above.

A CV of the WO_3/PB film in a 0.1 M KNO_3 aqueous solution is shown in Figure 5. The redox response of PW/PB was observed at 0.11 V, although it is overlapping the response of H_xWO_3/WO_3 below 0.28 V; however, the response of PB/BB was not observed in an oxidative scan up to 1.5 V. This

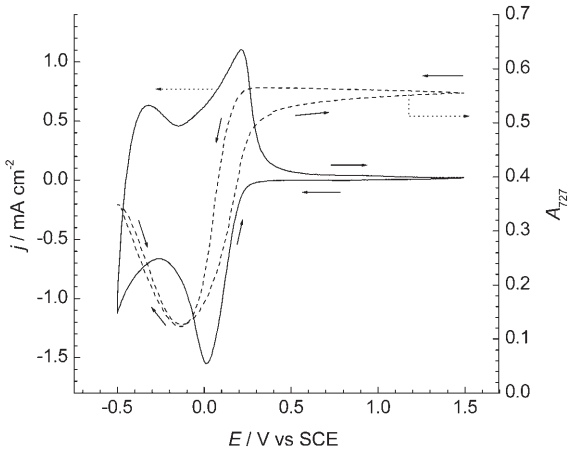

Figure 5. CV (solid line) and absorbance change at 727 nm (A_{727}; dashed line) in a SCV measurement of a WO_3/PB film in 0.1 M KNO_3 aqueous solution (pH 1.2), measured at 50 mV s^{-1}.

is also shown by the nondecreasing A_{727} at potentials over 0.8 V in the in situ absorption spectral change seen in Figure 6 and Supporting Information Figure S2 (two-dimensional representation, segmented into each reaction stage). To make correspondence between the absorption spectral change and the CV clearer, the potential profile of A_{727} is shown together with the CV in Figure 5. In the oxidative scan from −0.5 V, after A_{727} decreased initially by oxidation of H_xWO_3 to WO_3 with the anodic current, it then increased due to oxidation of PW to PB at −0.13 V, which is the same potential as the increase in the anodic current, and then remained constant to 1.5 V. In a reverse scan, A_{727} decreased at 0.28 V due to reduction of PB to PW, simultaneous with a rise in the cathodic current, finally coming back to the original value (before the potential scan) by reduction of WO_3 to H_xWO_3. From the potential profile of the A_{727} as well as the CV data, redox reactions based on PB for the WO_3/PB film are represented in Equation (3) under the potential conditions employed. However, they occur through H_xWO_3/WO_3 redox below the FB potential.

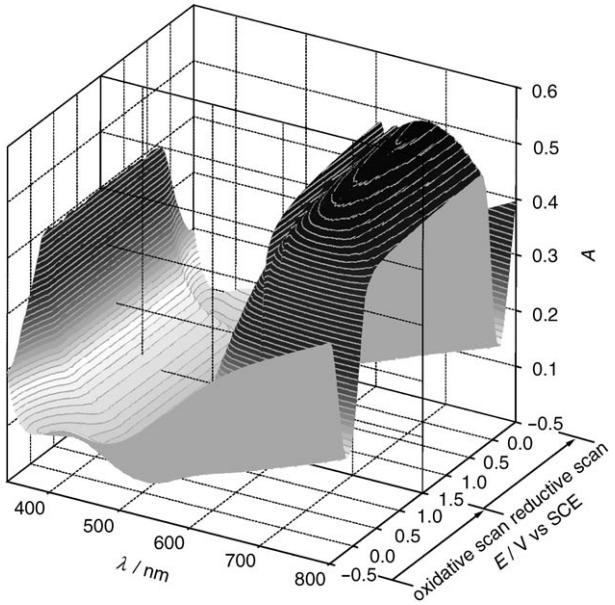

Figure 6. In situ absorption spectral change in a SCV measurement of a WO_3/PB film in 0.1 M KNO_3 aqueous solution (pH 1.2), measured at 50 mV s^{-1}.

$$Fe^{II}\text{-}Fe^{II}\ (PW) \underset{e^-}{\overset{-e^-}{\rightleftharpoons}} Fe^{II}\text{-}Fe^{III}\ (PB) \qquad (3)$$
$$0.11\ V$$

The redox behavior of the WO_3/PB film can be explained by the n-type Schottky heterojunction formed in an interface between the WO_3 and PB layers, as shown in the energy diagram and directed electron transfer of Scheme 1. PW can be oxidized to PB in an oxidative scan because its redox potential (0.14 V) is lower than the FB potential (0.26 V) of the WO_3 film. (Scheme 1A) However, oxidation of PB to BB requiring a much higher redox potential (0.86–1.10 V) than the FB potential is not allowed by the interfacial Schottky barrier, resulting in no further oxidation of PB under sufficiently high applied potentials. In the reverse reductive scan, PB is reduced to PW below its redox potential (0.14 V) (Scheme 1B).

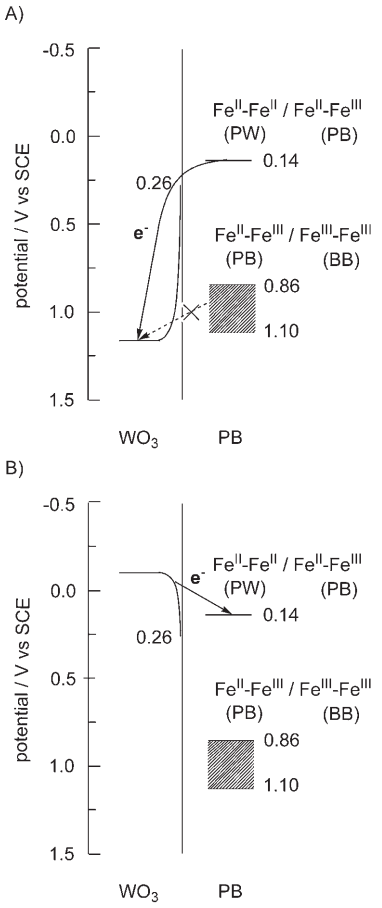

Scheme 1. A) and B): Energy diagrams and directed electron transfer suggested for the SCV measurements of a WO_3/PB film.

$[Ru(bpy)_3]^{2+}$-doped WO_3/PB film: A CV of the $[Ru(bpy)_3]^{2+}$-doped WO_3 film in a 0.1 M KNO_3 aqueous solution exhibits a reversible redox wave at 1.03 V on a Ru^{II}/Ru^{III} in a potential range from 0.5 to 1.5 V, as shown by the dashed line in Figure 7. The solid line in Figure 7 shows the corresponding CV in a 10 mM BB aqueous colloid solution during repetition of the potential scan. Both anodic and cathodic peak currents increased as the number of repetitions increased, indicating that the PB film is deposited from BB colloid onto the electrode coupled with the redox of Ru^{II}/Ru^{III}.

The $[Ru(bpy)_3]^{2+}$-doped WO_3/PB film prepared under the galvanostatic conditions of $-5\ \mu A\,cm^{-2}$ with $5\ mC\,cm^{-2}$ gave an absorption maximum at 716 nm, and the absorbance ($A_{716}=0.44$) provided $\Gamma_{PB}=6.7\times10^{-8}\ mol\,cm^{-2}$ for the [Ru-

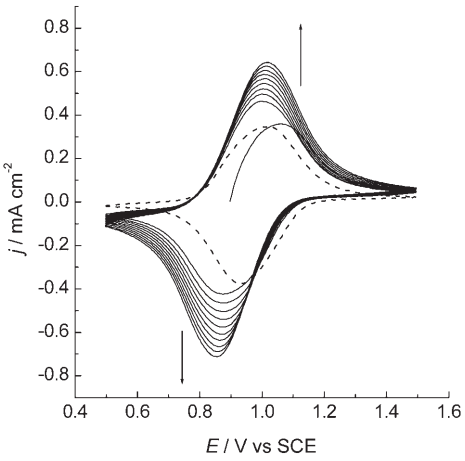

Figure 7. Repetitive CVs (solid line) of a $[Ru(bpy)_3]^{2+}$-doped WO_3 film in 10 mM BB aqueous solution, measured at 50 mV s^{-1}. Dashed line represents the CV of a $[Ru(bpy)_3]^{2+}$-doped WO_3 film in 0.1 M KNO_3 aqueous solution.

$(bpy)_3]^{2+}$-doped WO_3/PB film, calculated similarly to the WO_3/PB film. To evaluate a layer structure of the bilayer film using an AFM technique, a PB film was electrodeposited onto one half of the surface area of the $[Ru(bpy)_3]^{2+}$-doped WO_3 film, the other half masked with Teflon tape. A clear bilayer structure was corroborated by an AFM image at the boundary between the $[Ru(bpy)_3]^{2+}$-doped WO_3 surface (with masking) and the PB surface (without masking), showing a distinguishable step of the surface level at the boundary (Figure 8A). This result is consistent with the PB film layered on the WO_3 film. Figure 8B shows the height profile at the section between sites (a) and (b) in Figure 8A. The PB layer thickness is 70 nm, deduced from the difference in the surface levels. The AFM data was analyzed to give arithmetic mean values of surface roughness; $R_a = 2.90$ and 4.00 nm for the $[Ru(bpy)_3]^{2+}$-doped WO_3 surface and PB surface, respectively, revealing that the latter is rougher than the former. This might be related to the particle sizes of PTA and BB colloid, the precursors for electrodeposition of the former and latter, respectively.

A CV of the $[Ru(bpy)_3]^{2+}$-doped WO_3/PB film in a 0.1 M KNO_3 aqueous solution is shown by the solid line in Figure 9. The electrochemical response assigned to the redox of PB was not observed in the CV, although redox responses of Ru^{II}/Ru^{III} and H_xWO_3/WO_3 were observed at 1.03 V and below 0.09 V, respectively. However, the anodic peak current at 1.2 V, as well as the cathodic current at −0.5 V, are higher than the corresponding current values for the CV of the $[Ru(bpy)_3]^{2+}$-doped WO_3 film (without a PB film). The CV in Figure 9 did not change during a repetitive potential scan of more than ten cycles from −0.5 to 1.5 V, indicating that all the redox reaction is reversible in the potential range employed. Upon scanning the potential from 0.5 to 1.5 V, the high anodic peak current at 1.2 V relative to the corresponding cathodic peak current was also observed in the first scan, but the anodic peak current decreased in the second scan, to be comparable with the cathodic peak

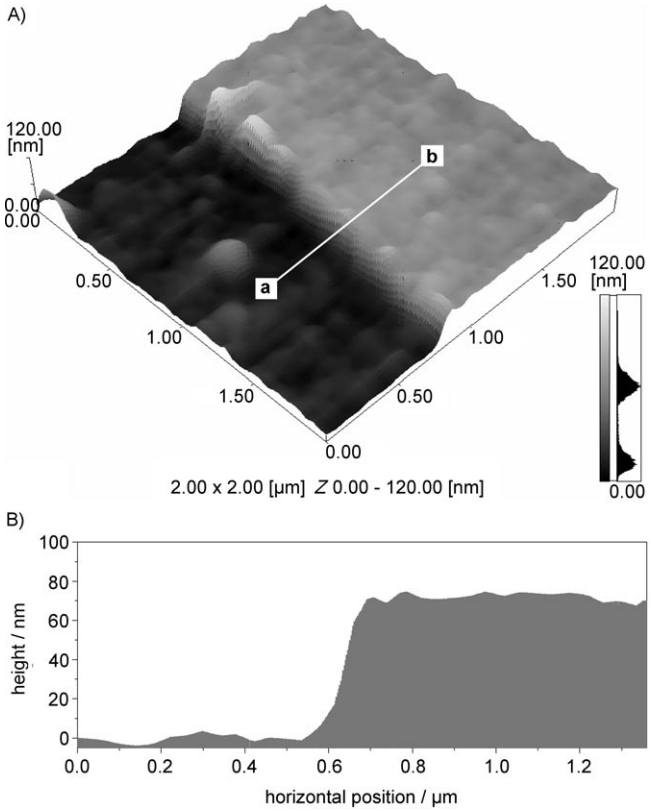

Figure 8. A) AFM image of the boundary between a $[Ru(bpy)_3]^{2+}$-doped WO_3 surface and the layered PB surface. The PB film was electrodeposited onto one half of the surface area of the $[Ru(bpy)_3]^{2+}$-doped WO_3 film, the other half masked with Teflon tape. Site a is on the $[Ru(bpy)_3]^{2+}$-doped WO_3 surface, and site b is on the layered PB surface. B) Height profile at the section between sites a and b. The horizontal position on the x-axis represents the distance from site a.

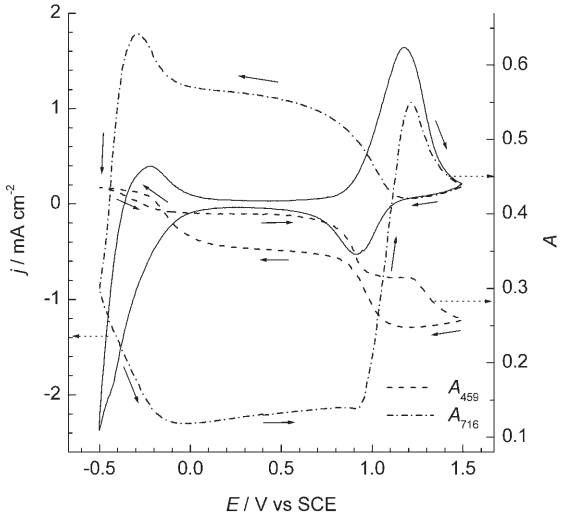

Figure 9. CV (——) and absorbance changes at 459 nm (A_{459}; -----) and 716 nm (A_{716}; –•–•–) in a SCV measurement of a $[Ru(bpy)_3]^{2+}$-doped WO_3/PB film in 0.1 M KNO_3 aqueous solution (pH 1.2), measured at 50 mV s^{-1}.

current (Supporting Information Figure S3). Notably, in comparison with CV (Figure 5) of the WO_3/PB film, the redox response of PW/PB at 0.11 V disappeared for the $[Ru(bpy)_3]^{2+}$-doped WO_3/PB film. This is ascribed to the $[Ru(bpy)_3]^{2+}$ doping causing a decrease in FB potential of WO_3 to a potential (0.09 V) that is significantly lower than the redox potential (0.14 V) of PW/PB.[13]

To reveal the electrochemical reactions for the $[Ru(bpy)_3]^{2+}$-doped WO_3/PB film, an in situ absorption spectral change was recorded simultaneously with its CV measurement. The in situ absorption spectral change (Figure 10, and

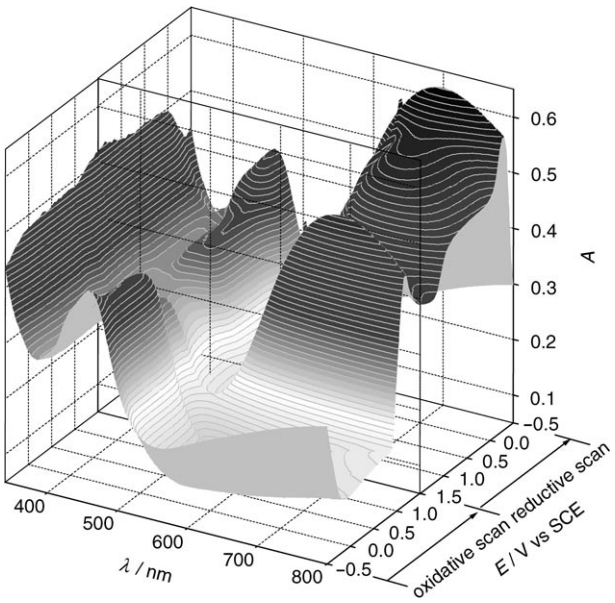

Figure 10. In situ absorption spectral changes in a SCV measurement of a $[Ru(bpy)_3]^{2+}$-doped WO_3/PB film in 0.1 M KNO_3 aqueous solution (pH 1.2), measured at 50 mV s^{-1}.

Supporting Information Figure S4 as a two-dimensional representation, segmented into each reaction stage) clearly exhibited the generation of an intense and broad absorption band at 716 nm, attributed to PB at around 1.0 V in an oxidative scan (though the redox response assigned to oxidation of PW to PB was not indicated in the CV data), in addition to the absorbance changes at 459 nm and at >450 nm for Ru^{II} and H_xWO_3, respectively. To correlate the absorbance data to electrochemical reactions, the potential profiles of absorbances at 459 nm (A_{459}; mainly due to Ru^{II}) and at 716 (A_{716}; mainly due to PB and H_xWO_3) are shown together with the corresponding CV in Figure 9. In an oxidative scan from −0.5 V, A_{716} decreased by oxidation of H_xWO_3 to WO_3, maintaining an almost constant value of 0.11–0.12 above −0.1 V. A_{459} started to decrease at 0.9 V by oxidation of Ru^{II} to Ru^{III} and then remained constant from 0.95 V to 1.2 V, whereas A_{716} increased by formation of PB at the same potential (0.95 V). The linked profiles of A_{716} and A_{459} indicate that PW is oxidized to PB by Ru^{III} formed electrochemically. A_{459} decreased again in synchronization with the A_{716} decrease after A_{716} reached the maximum (0.55) at 1.2 V. The A_{716} decrease is due to oxidation of PB to BB, and the synchronization of A_{459} and A_{716} suggests that PB is also oxidized to BB by Ru^{III}. These results imply that the anodic wave at 1.2 V for the CV includes three oxidation reactions of Ru^{II} to Ru^{III}, PW to PB, and successive oxidation of PB to BB, the latter two of which take place by a geared reaction of Ru^{II}/Ru^{III}. The decrease (0.15) of A_{459} as well as the increase (0.41) and the subsequent decrease (0.13) of A_{716} gave 1.0, 6.2, and 2.0×10^{-8} mol cm^{-2} for the oxidized amounts of Ru^{II}, PW, and PB, respectively, by using $\varepsilon_{Ru^{II}}=14\,600$ M^{-1} cm^{-1} and $\varepsilon_{PB}=6600$ M^{-1} cm^{-1}. The amount (6.2×10^{-8} mol cm^{-2}) of PW oxidized is 93% of Γ_{PB} (6.7×10^{-8} mol cm^{-2}) on the electrode, which indicates that nearly all PW is oxidized to PB by the geared reaction of Ru^{II}/Ru^{III}. The amount (2.0×10^{-8} mol cm^{-2}) of PB oxidized indicates that 32% of PB formed is oxidized to BB by the geared reaction. The total amount (9.2×10^{-8} mol cm^{-2}) of Ru^{II}, PW, and PB oxidized is consistent with the charge amount (8.9 mC cm^{-2}) in the anodic wave.

During a reverse reductive scan, A_{716} increased at 1.1 V, synchronized with the A_{459} increase, showing the reversible reduction of BB to PB coupled with the Ru^{II}/Ru^{III} redox. This could be explained by the coupled redox equilibria involving rapid-exchange electron transfer among the redox pairs. During the further reductive scan, A_{716} maintained a nearly constant value of 0.56–0.57, and after increasing at −0.2 V due to reduction of WO_3 to H_xWO_3, it decreased at −0.5 V to the original A_{716} value (before the potential scan), suggesting that reduction of PB to PW takes place by reduction of WO_3 to H_xWO_3. The potential profile of A_{716} exhibited significant hysteresis based on the PW/PB redox in the range of −0.1–0.9 V, in which A_{716} (0.56–0.57) in the reductive scan is five times higher than that (0.11–0.12) in the anodic scan by formation of PB, as shown by a dot-and-dash line in Figure 9. The electrochromic hysteresis performance is caused by the electrochemical reactions geared by Ru^{II}/Ru^{III} (for oxidation of PW) and H_xWO_3/WO_3 (for reduction of PB), as shown in Scheme 2.

The energy diagrams and directed electron transfers for the $[Ru(bpy)_3]^{2+}$-doped WO_3/PB film are summarized in Scheme 3. The n-type Schottky heterojunction could be formed in the interface between WO_3 and PB film for the

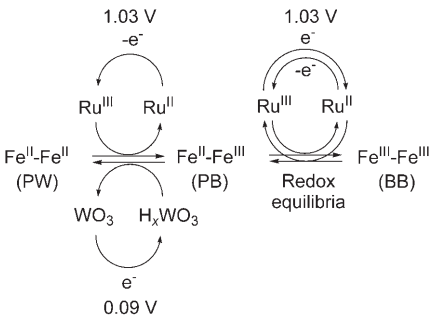

Scheme 2. Electrochemical geared cycle reactions for a $[Ru(bpy)_3]^{2+}$-doped WO_3/PB film.

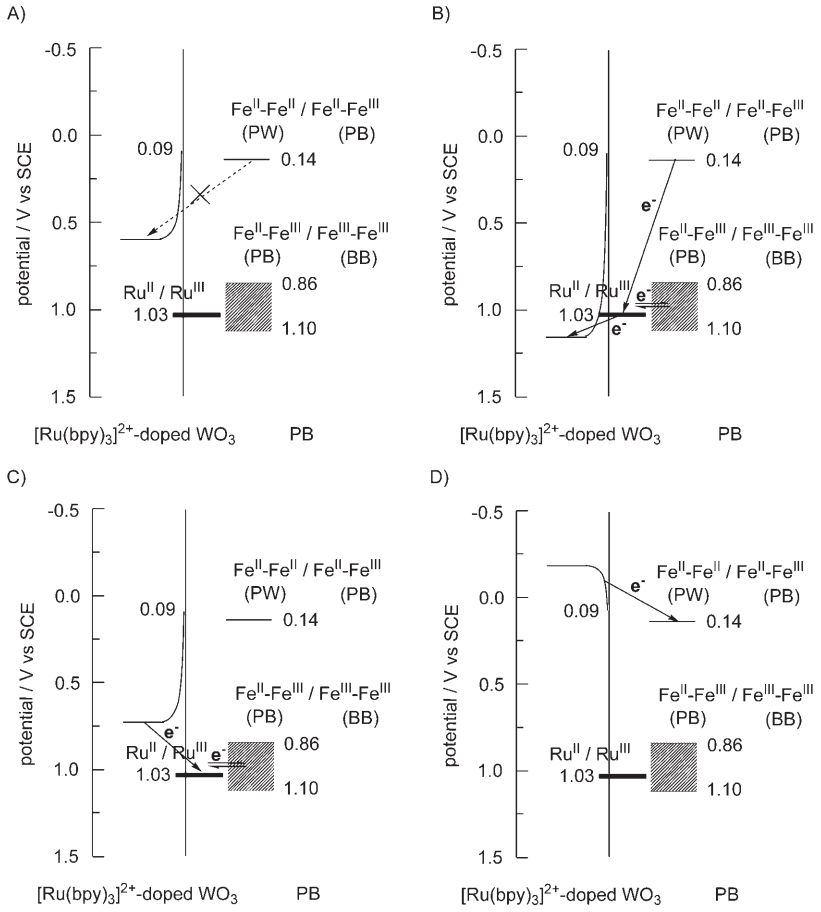

Scheme 3. A)–D) Energy diagrams and directed electron transfer suggested for the SCV measurements of a $[Ru(bpy)_3]^{2+}$-doped WO_3/PB film.

$[Ru(bpy)_3]^{2+}$-doped WO_3/PB film, similar to the WO_3/PB film. If the electrode potential is higher than the redox potential (0.14 V) of the PW/PB, electron transfer from PW to the conduction band of WO_3 is not allowed by the Schottky barrier, because the FB potential (0.09 V) is lower than the redox potential (0.14 V) of PW/PB (Scheme 3A). As the electrode potential becomes higher than 1.03 V, Ru^{II} can be oxidized to Ru^{III} because the ohmic contact is formed between WO_3 and $[Ru(bpy)_3]^{2+}$. Upon oxidation of Ru^{II}, electrons are rapidly transferred from PW to the Ru^{III} formed, resulting in the high anodic peak current (due to oxidation of Ru^{II}) at 1.2 V in the CV in Figure 9 (Scheme 3B). The redox potential of PB/BB has a relatively broad energy level (see CV in Figure 2) and is very close to that for Ru^{II}/Ru^{III}, which enables the two redox reactions to be coupled to each other by equilibria involving rapid-exchange electron transfer among the redox couples. The coupled redox equilibria results in the electrochemical reaction of PB/BB synchronized with the Ru^{II}/Ru^{III} redox. As the electrode potential is reductively scanned to 0.5 V, Ru^{III} is reduced to Ru^{II} and coupled to the reduction of BB to PB (Scheme 3C). As it is reversed again from 0.5 to 1.5 V, Ru^{II} is oxidized to Ru^{III}, coupled to the oxidation of PB to BB, however, electron transfer does not take place from PW to Ru^{III} because nearly all PW is already oxidized to PB during the first scan to 1.5 V. As the potential becomes lower than the FB potential (0.09 V) of WO_3, PB can be re-reduced to PW because the reduction of PB to PW requires the geared reaction by H_xWO_3/WO_3 (Scheme 3D).

Conclusion

$[Ru(bpy)_3]^{2+}$ was doped in a WO_3 film by using an electrodeposition technique to form an electron-transfer channel in which the Ru^{II}/Ru^{III} redox passes through an n-type Schottky barrier at an interface between a WO_3 film and an electrolyte solution. This is a very unique feature in interfacial chemistry related to heterojunctions of semiconductors. Electron transfer from the ground state of $[Ru(bpy)_3]^{2+}$ confined in the film to the conduction band of WO_3 was effectuated by the unique electron-transfer channel, in contrast to electron transfer from the excited state of dye molecules to the conduction band of TiO_2 at a liquid heterojunction for dye-sensitized solar cells. A new electrochromic $[Ru(bpy)_3]^{2+}$-doped WO_3/PB bilayer film was developed by a two-step electrodeposition procedure. The redox of the PB film layered was controlled by $[Ru(bpy)_3]^{2+}$-doped WO_3/PB in which an electron-transfer channel passing through the interfacial Schottky barrier is formed by the Ru^{II}/Ru^{III} redox. The controlled electron transfer produced a unique and novel electrochromic hysteresis performance based on PW/PB. This unique performance may be applicable to a large variety of promising electronic devices, such as memory, display, and switching devices. The photochemical reactivity of $[Ru(bpy)_3]^{2+}$ affords the possibility of photoswitching of the PW/PB states, based on the hysteresis performance. We are undertaking extended studies on photoswitching of the PW/PB states for the $[Ru(bpy)_3]^{2+}$-doped WO_3/PB bilayer film for use in a photowriting and electroerasing device.

Experimental Section

Materials: $[Ru(bpy)_3]Cl_2 \cdot 6H_2O$ and PSS (Mw = 70000) were purchased from Aldrich. Tungsten powder, hydrogen peroxide (30%) and $FeCl_3 \cdot 6H_2O$ were purchased from Kanto Kagaku. $K_3[Fe(CN)_6]$ was purchased from Wako Pure Chemicals. All reagents were used as received.

Preparations

WO_3 film: Tungsten powder (0.92 g, 5.0 mmol) was dissolved in 30% hydrogen peroxide to produce a PTA solution. After excess hydrogen peroxide was decomposed by Pt black, ethanol was added to the solution to stabilize PTA to give a final aqueous ethanol solution (30 vol%) containing 100 mM PTA (based on W concentration) as a stock solution. A WO_3 film was electrodeposited onto an ITO electrode from an aqueous ethanol solution (30 vol%) containing 50 mM PTA and 30 mM PSS with stirring under the potentiostatic conditions (−0.45 V vs Ag/AgCl) to 1.0 C cm^{-2}, by using a conventional single-compartment electrochemical cell equipped with an ITO working electrode, an Ag/AgCl reference electrode, and a platinum-wire counter electrode. The prepared film was cathodically polarized at −0.5 V vs SCE in a 0.1 M HNO_3 aqueous solution to complete the electrodeposition of PTA.

$[Ru(bpy)_3]^{2+}$-doped WO_3 film: $[Ru(bpy)_3]^{2+}$ and PSS solutions were added to the PTA solution to prepare an aqueous ethanol solution (30 vol%) containing 1 mM $[Ru(bpy)_3]^{2+}$, 50 mM PTA, and 30 mM PSS. After standing the solution at room temperature, it turned into a colloidal triad solution of $[Ru(bpy)_3]^{2+}$, PTA, and PSS. A $[Ru(bpy)_3]^{2+}$-doped WO_3 film was electrodeposited from the colloidal triad solution onto an ITO electrode under the same conditions as for preparation of the WO_3 film to 1.0 C cm^{-2}, and then treated by cathodic polarization at −0.5 V vs SCE in a 0.1 M HNO_3 aqueous solution. The X-ray diffraction measurement indicated amorphous WO_3 in the $[Ru(bpy)_3]^{2+}$-doped WO_3 film. The thickness of the formed film was measured by a scanning electron microscopic technique to be 560 (±24) nm (on average). The UV/Vis spectroscopic measurement indicated that $[Ru(bpy)_3]^{2+}$ is uniformly confined in the film, and the coverage of $[Ru(bpy)_3]^{2+}$ was calculated to be 3.4×10^{-8} mol cm^{-2} from the absorbance at $\lambda_{max} = 459$ nm and $\varepsilon_{Ru^{II}} = 14600\ M^{-1}\,cm^{-1}$.

PB film, WO_3/PB film, and $[Ru(bpy)_3]^{2+}$-doped WO_3/PB film: A colloidal aqueous solution of 10 mM BB was prepared from the aqueous solution containing 10 mM $FeCl_3$ and 10 mM $K_3[Fe(CN)_6]$. PB was cathodically electrodeposited from the colloidal solution onto an ITO, WO_3 film, or $[Ru(bpy)_3]^{2+}$-doped WO_3 film under galvanostatic conditions of −5 to −50 μA cm^{-2} to 5 to 10 mC cm^{-2} to prepare a PB film, a WO_3/PB film, or a $[Ru(bpy)_3]^{2+}$-doped WO_3/PB film, respectively.

Measurements: SCV measurements were conducted by combining a photodiode array spectrophotometer (Shimadzu, Multispec-1500) with a potentiostat (Hokuto Denko, HA-501G) and a function generator (Hokuto Denko, HB-104). A conventional single-compartment electrochemical cell was equipped with a modified working electrode, an SCE reference electrode, and a platinum-wire counter electrode. AFM measurements were carried out in contact mode by using an AFM microscope (Shimadzu, SPM-9500 J3).

Acknowledgements

Research was partially supported by Grant-in-Aid for Young Scientists (B) from the Ministry of Education, Culture, Sports, Science, and Technology (No. 16750113) and Grant for Promotion of Niigata University Research Projects. A fellowship grant was provided by The Niigata Engineering Promotion (K.S.).

[1] R. Memming, *Semiconductor Electrochemistry*, Wiley-VCH, Weinheim, **2001**.
[2] J. Gordon, E. Brown, V. E. Henrich, W. H. Casey, D. L. Clark, C. Eggleston, A. Felmy, D. W. Goodman, M. Grätzel, G. Maciel, M. I. McCarthy, K. H. Nealson, D. A. Sverjensky, M. F. Toney, J. M. Zachara, *Chem. Rev.* **1999**, *99*, 77–174.
[3] A. J. Bard, L. R. Faulkner, *Electrochemical Methods: Fundamentals and Applications*, John Wiley & Sons, New York, **2001**.
[4] A. Fujishima, K. Hashimoto, T. Watanabe, *TiO_2 Photocatalysis, Fundamentals and Applications*, BKC, Tokyo, **1999**.
[5] B. O'Regan, M. Grätzel, *Nature* **1991**, *353*, 737–740.
[6] M. Grätzel, *Inorg. Chem.* **2005**, *44*, 6841–6851.
[7] C. Santato, M. Ulmann, J. Augustynski, *Adv. Mater.* **2001**, *13*, 511–514.
[8] C. Santato, M. Odziemkowski, M. Ulmann, J. Augustynski, *J. Am. Chem. Soc.* **2001**, *123*, 10639–10649.
[9] C. G. Granqvist, *Sol. Energy Mater. Sol. Cells* **2000**, *60*, 201–262.
[10] D. L. Bellac, A. Azens, C. G. Granqvist, *Appl. Phys. Lett.* **1995**, *66*, 1715–1716.
[11] S.-H. Baeck, K.-S. Choi, T. F. Jaramillo, G. D. Stucky, E. W. McFarland, *Adv. Mater.* **2003**, *15*, 1269–1273.
[12] A. Juris, V. Balzani, F. Barigelletti, S. Campagna, P. Belser, A. von Zelewsky, *Coord. Chem. Rev.* **1988**, *84*, 85–277.
[13] M. Yagi, K. Sone, M. Yamada, S. Umemiya, *Chem. Eur. J.* **2005**, *11*, 767–775.
[14] M. Yagi, S. Umemiya, *J. Phys. Chem. B* **2002**, *106*, 6355–6357.
[15] K. Itaya, T. Ataka, S. Toshima, *J. Am. Chem. Soc.* **1982**, *104*, 4767–4772.
[16] D. Ellis, M. Eckhoff, V. D. Neff, *J. Phys. Chem.* **1981**, *85*, 1225–1231.
[17] M. B. Robin, *Inorg. Chem.* **1962**, *1*, 337–342.
[18] M. Kaneko, S. Teratani, K. Harashima, *J. Electroanal. Chem.* **1992**, *325*, 325–332.
[19] K. Itaya, I. Uchida, V. D. Neff, *Acc. Chem. Res.* **1986**, *19*, 162–168.

Received: March 13, 2006
Published online: August 25, 2006

